Publications of the Astronomical Society of the Pacific
105: 881–893, 1993 August

The Sandiford 2.1-m Cassegrain Echelle Spectrograph for McDonald Observatory: Optical and Mechanical Design and Performance

JAMES K. MCCARTHY, BRENDAN A. SANDIFORD, DAVID BOYD, AND JOHN BOOTH

McDonald Observatory, The University of Texas at Austin, R. L. M. 15.308, Austin, Texas 78712
Electronic mail: jkm@deimos.caltech.edu

Received 1993 February 22; accepted 1993 May 10

ABSTRACT. We describe the design, construction, and performance of an efficient new flexure-compensated Cassegrain echelle spectrograph for the 2.1-m (82-in.) Struve reflector at McDonald Observatory. The instrument has a resolving power $R=\lambda/\Delta\lambda$ of 60,000 for two CCD pixels (for a reciprocal velocity dispersion of 2.5 km s^{-1} per pixel) and provides continuous wavelength coverage for $\lambda<8000$ Å using a thinned backside-illuminated Reticon 1200×400 CCD detector. Total wavelength coverage in a single exposure varies from roughly 500 Å at $\lambda=4400$ Å (range 4200–4700 Å) to 2500 Å at $\lambda=7500$ Å (range 6500–9000 Å), and the total system efficiency at $\lambda=6000$ Å from the top of the atmosphere through the telescope, spectrograph, and CCD detector is 10% or more. The mechanical design of the Cassegrain-mounted spectrograph incorporates a unique cantilevered counterweight system designed to drastically reduce the effects of gravitational flexure. In spite of the large physical size of the Cassegrain instrument, worst-case flexure shifts over 60° (4 hr) of telescope motion are less than $\frac{1}{2}$ pixel and are typically on the order of 0.2 pixels or less from all sources. A subsequent paper will describe the CCD and associated electronics in detail.

1. INTRODUCTION

High-resolution optical spectroscopy of late-type stars has been and continues to be one of the primary research activities at McDonald Observatory (e.g., Lambert 1991; Smith 1988; Sneden 1991; Smith 1991). Detailed abundance analyses and/or radial-velocity measurements of the resulting high S/N, high dispersion spectra provide important clues to the nature of the stars under study: whether single or binary, their temperatures, luminosities, chemical compositions, and evolutionary history of nucleosynthesis and convective dredge up, to name a few. Until recently, however, the observational data required to carry out such research was acquired using either of the coudé spectrographs of the 2.1- or 2.7-m telescopes (Hiltner 1949 and Tull 1972, respectively) to record part of a single diffracted order from a large 1200 gr mm^{-1} grating (or for higher resolution, part of a single order from an echelle grating, with the penalty of even less spectral coverage per exposure). Stellar photons with wavelengths outside the ~100 Å or less of the spectrum imaged onto the CCD detector were lost, and multiple exposures of the same objects at different wavelength settings were required to carry out many research programs. These factors combined with the typically narrow slits necessary to achieve the requisite spectral resolution meant that the overall efficiency with which clear nights of telescope time were used was unavoidably low.

Therefore, we set out in 1989 to design and build a cross-dispersed CCD echelle spectrograph for the McDonald 2.1-m telescope, based on the success of an efficient $R=\lambda/\Delta\lambda=20{,}000$ Cassegrain echelle spectrograph in use on the 1.5-m telescope at Palomar Observatory (McCarthy 1985, 1988). Design and fabrication of a large coudé cross-dispersed echelle spectrograph for the McDonald 2.7-m was already underway (MacQueen and Tull 1988; Tull and MacQueen 1988; Tull et al. 1993), and coudé or Cassegrain cross-dispersed echelle spectrographs were in use or coming on-line at other observatories including Pine Bluff (Schroeder 1967), McGraw-Hill (Bardas 1977), the MMT (Chaffee and Latham 1982), Las Campanas (Shectman 1983–87), KPNO and CTIO (Pilachowski et al. 1982; York et al. 1981; Ramsey and Huenemoerder 1986), Lick (Vogt 1987, 1988), ARC (Schroeder 1988), the AAT and WHT (Walker 1988; Diego, 1988; Diego et al. 1991), ESO (le Luyer et al. 1979; Enard 1982), and Keck (Vogt and Penrod 1988). These instruments have in common the use of a diffraction grating (the echelle) in very high orders to provide high dispersion, coupled with either a low-order grating or one or more prism "cross dispersers" to separate the otherwise overlapping orders from the echelle grating (Schroeder 1970). Echelle spectrographs are therefore able to combine high resolution (in any one echelle order) with large wavelength coverage owing to the fact that many orders are recorded simultaneously on a two-dimensional detector such as a CCD.

For maximum possible throughput efficiency, we chose to design a Cassegrain instrument rather than one at coudé (where four mirrors are required to reach the slit through the cross-axis mount of the 2.1-m Struve Telescope). Fiber-optic coupling of a Cassegrain instrument to the telescope focus (Barden 1988; Ramsey 1988) would provide an alternate mode of operation in cases where concerns for utmost stability outweigh efficiency considerations. Fiber-optic coupling would also enable the presumably large 2.1-m Cassegrain instrument to be used with the relatively

undersubscribed McDonald Observatory 0.9-m telescope in the future.

2. OPTICAL DESIGN PARAMETERS

2.1 CCD Detector Dimensions

The scientific objective of detailed abundance determinations for late-type stars required that the new instrument provide a resolution of at least 60,000 and continuous wavelength coverage (wavelength overlap between orders, not gaps) in a single exposure, if possible. Financial constraints essentially ruled out monochromatic beam diameters larger than 150 mm, and TEK2048 CCDs. However, large CCD pixels and a large number of CCD pixels in the dispersion direction remained important criteria in meeting our design goals. Therefore, we decided early on to match the spectrograph format to the Reticon 1200×400 CCD array with 27 μm pixels (Tseng et al. 1989; Cizdziel 1990; Gilmore et al. 1990; Geary et al. 1990; Robinson et al. 1991) which offered state-of-the-art CTE and read-noise performance ($\simeq 4\ e^-$ rms) and was commercially available thinned and backside illuminated for optimum QE all at a reasonable cost.

2.2 Camera and Collimator Dimensions

The camera effective focal length ($\mathrm{EFL_{cam}}$) required to yield a given resolution (R) can be expressed in terms of the grating dispersive power ($\lambda d\beta/d\lambda$) and image size (Δx) on the detector as follows:

$$R=\frac{\lambda}{\Delta\lambda}=\lambda\frac{d\beta}{d\lambda}\left(\frac{\mathrm{EFL_{cam}}}{\Delta x}\right)=60{,}000, \qquad (1)$$

where for an R2 echelle grating with blaze angle $\theta_B=63°26'$, the dispersive power $\lambda d\beta/d\lambda=4.167$. For a slit width projecting onto two 27 μm pixels, $\Delta x=54$ μm and thus from Eq. (1), $\mathrm{EFL_{cam}}=(4.167)^{-1}(60{,}000)(0.054\ \mathrm{mm})=777$ mm $\simeq 30$ in. The collimator focal length required in order for the slit width Δw to project to an image size Δx is simply $\mathrm{EFL_{coll}}=(\Delta w/\Delta x)\times\mathrm{EFL_{cam}}$ in the absence of significant anamorphic demagnification. One arcsecond at the $f/13.5$ Cassegrain of the 2.1-m Struve reflector corresponds to a linear measure $\Delta w=139$ μm, implying $\mathrm{EFL_{coll}}\simeq 2000$ mm in order to match a 1 arcsec slit to two CCD pixels. The spectrograph beam diameter follows from equating collimator and telescope f/ratios: $D_{\mathrm{coll}}=2000\ \mathrm{mm}/13.5=148$ mm $\simeq 6$ in., very large by 2.1-m Cassegrain spectrograph standards. Compactness of the spectrograph optical layout thus became a crucial concern in the design (see Sec. 3.1).

2.3 Dispersing Elements

The free spectral range of an echelle grating has an angular extent given by

$$\Delta\beta(\mathrm{m})=\frac{\lambda_c}{a\cos\beta_c\cos\gamma}$$
$$=\frac{\lambda_c}{a\cos\theta_B},\ \gamma=0,\ \beta_c=\theta_B$$
$$=\frac{2\tan\theta_B}{m},\ \alpha=\beta_c=\theta_B, \qquad (2)$$

where λ_c is the central wavelength of order number m, angles α, β, and γ are the standard grating angles, β_c is the value of grating angle β at order center, and a is the groove spacing of the echelle grating. The second of these equations can be rewritten $\Delta\beta(m)=1.28°(N/10)(\lambda_c/10^4\ \text{Å})$, where $N=a^{-1}$ in grooves mm^{-1}. For $\lambda_c=8000$ Å and $N=31.6$ gr mm^{-1}, we find $\Delta\beta=3.24°$, which exceeds the 2.39° angular extent of the 1200 pixel Reticon CCD in the focal plane of 30 in. focal length camera, and indeed gaps would exist in the wavelength coverage of a single exposure at wavelengths longer than 5900 Å with the 31.6 gr mm^{-1} echelle grating.

Discussions with Milton Roy revealed their interest in a new 154×306 mm R2 echelle master with 23.2 gr mm^{-1}, to replace the recently discontinued 128×254 mm 23.2 gr mm^{-1} R2 echelle submaster from the now retired Kitt Peak "C" engine (Loewen 1988). We therefore selected this coarse echelle ruling as the basis for our spectrograph design, as it provides continuous wavelength coverage for $\lambda\leqslant 8000$ Å at a two pixel resolution of $R=60{,}000$ with the Reticon 1200×400 CCD detector.

It is well known that prism cross dispersers provide a more uniform order-to-order separation than low-order grating cross dispersers, since the decrease in the echelle grating free spectral range toward the shorter wavelengths is more than compensated for by an increase in prism dispersion toward the blue. Furthermore, low-order grating cross dispersers are generally less efficient and introduce their own blaze functions, decreasing efficiency further at extreme wavelengths. After running numerical experiments for several different prism materials and apex angles, we decided upon a 40° apex angle LF5 prism placed in front of the echelle grating and used in double pass (or equivalently a pair of such prisms used in single pass) as an overall compromise between adequate dispersion (the coarse 23.2 gr mm^{-1} echelle grating has a very small free spectral range; i.e., small wavelength difference between adjacent orders), small apex angle (minimizing reflection losses as well as the total path length through glass), near-UV transmission (25 mm of LF5 transmits 95.5% at $\lambda=3650$ Å), and cost.

Figure 1 shows the predicted output spectrum format of the 23.2 gr mm^{-1} R2 echelle grating, double-pass 40° apex LF5 prism, and a 30 in. EFL camera onto the Reticon 1200×400 CCD detector. Note that Fig. 1 extends vertically four times the 400 pixel CCD dimension, and for $\lambda\leqslant 8000$ Å wavelength coverage is continuous between the row 1 and row 400 wavelength limits of the CCD detector, whose y position in Fig. 1 can be smoothly varied to record the precise wavelength range of interest. Spacing between order centers is 10 pixels at $\lambda=1$ μm ($m=76$; Fig. 1 y

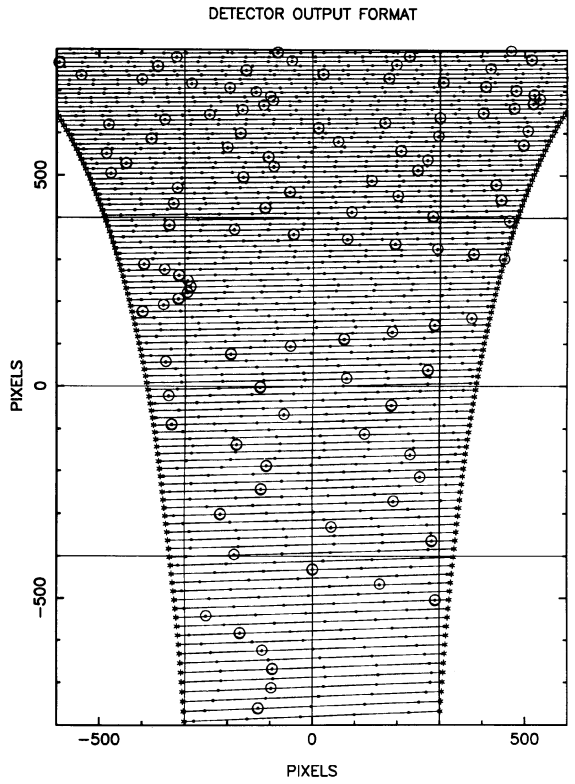

FIG. 1—CCD echelle image format resulting from the combined use of a 23.2 gr mm^{-1}R2 echelle grating with $2\theta=2.31°$, and a 40° apex angle LF5 prism used in double pass. The Reticon CCD used in the spectrograph measures 1200 columns (the width of this figure) by 400 rows (one fourth the height of this figure). Wavelength increases from left to right and from bottom to top. At the top is $\lambda=1$ μm($m=77$), at center is $\lambda=5506$ Å($m=140$), and at bottom is $\lambda=4281$ Å($m=180$).

position = +793), 13 pixels at $\lambda=6588$ Å ($m=117$; y position = +334), 16 pixels at 5506 Å ($m=140$; y position = 0), 20 pixels at 4758 Å ($m=162$; y position = −392), and 23 pixels at 4305 Å ($m=179$; y position = −756); as built, 2.0 CCD pixels correspond to 1.1 arcsec on the sky at the slit. Dots in Fig. 1 mark wavelengths which are multiples of 5 Å and circles multiples of 50 Å, while asterisks indicate the end of the free spectral range of each order. Beyond these positions the orders continue until reaching the edge of the CCD, and in fact the resulting wavelength overlap is essential when reconstructing the spectrum from the extracted orders (Gehren 1990).

3. OPTICAL DESIGN DETAILS

3.1 Spectrograph Optical Layout

In order to achieve the desired $R=60{,}000$ two pixel resolution, the first-order calculations in Sec. 2.2 above indicated a moderate camera f/ratio of $f/5$ is required, but a large beam diameter is necessary causing concern about the overall size of a Cassegrain instrument. After exploring many possible optical layouts, and with confidence that the optical performance of an $f/5$ camera lens system could be very high, we arrived at a configuration similar to that of the Las Campanas 2.5-m Dupont Telescope echelle spectrograph (Shectman 1983–87; also Shectman and McCarthy 1983) in which both the prism cross disperser *and the camera lens* are used in double pass. Small lenses (a postslit negative lens in the Dupont instrument; preslit positive lenses in our design, for reasons explained in Sec. 3.3 below) are employed to increase the speed of the input beam to match that of the camera and create the proper collimator effective focal length, EFL_{coll}. Our optical layout is shown in Fig. 2. The echelle grating is illuminated very close to true Littrow ($\alpha-\beta_c=2\theta=2.31°$), and in addition to its overall simplicity and compactness, the design minimizes the camera-to-grating distance thereby minimizing the unvignetted aperture of the camera lens required. By placing the ~45° folding mirror in the input beam below the slit, the long axis of the spectrograph runs radially along the underside of the telescope primary (rather than axially away from it), leading to a generally stiffer Cassegrain instrument (see Sec. 4).

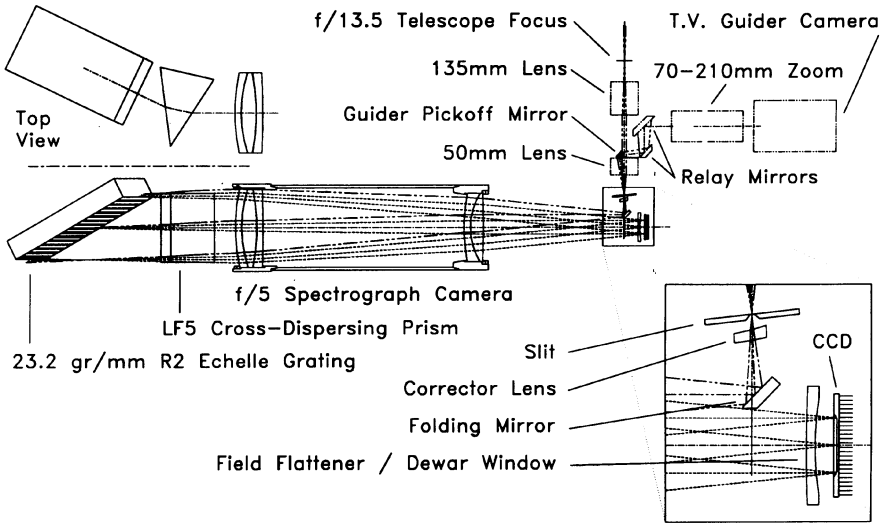

FIG. 2—Optical layout of the 2.1-m Cassegrain echelle spectrograph; note that the $f/5$ camera lens is used in double pass. See text for details.

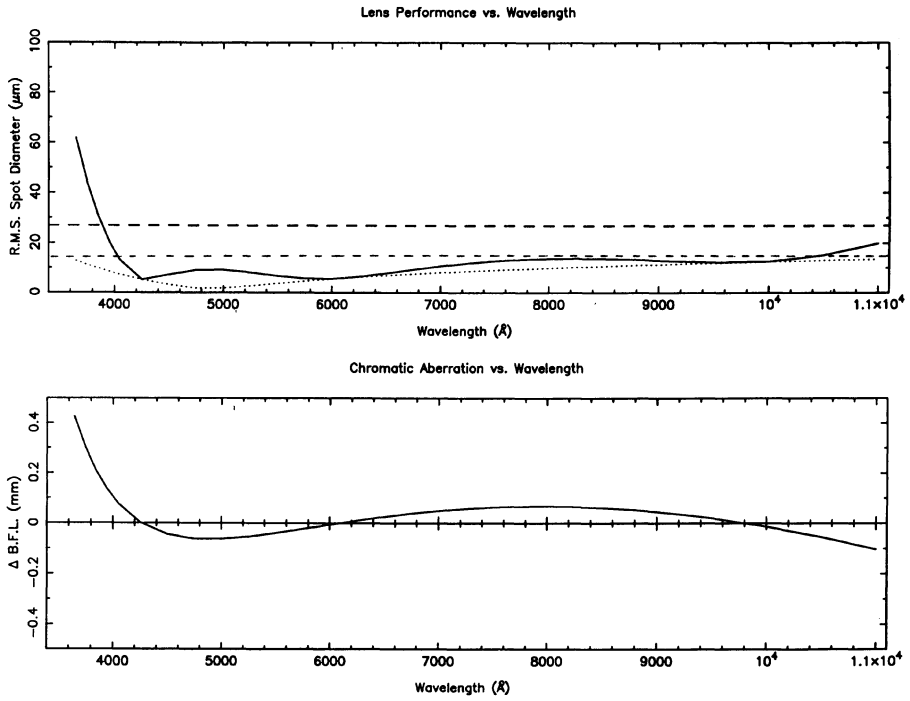

FIG. 3—Optical design performance of the 30 in. focal length camera lens design as a function of wavelength. Top: on-axis rms spot diameters are compared to representative 27 and 15 μm pixel sizes (horizontal dashed lines). Bottom: change in back focal length as a function of wavelength owing to chromatic aberration.

3.2 Camera Lens System

The camera lens system consists of a 190 mm aperture BaK2/CaF_2/SK15 cemented triplet lens followed by a 165 mm SK20/FK01 cemented doublet. This configuration of glasses was suggested by Dr. Harlan Epps (1989b) and represents a slower version of a more complex $f/3$ design (Epps 1989a) consisting of three airspaced doublets, two of which contain fluorite. Epps' design was fine tuned by one of us (J. K. M.) with the addition of a negative meniscus fused quartz field flattener (also to serve as CCD Dewar window) and reoptimized over the flat CCD focal plane and field size. All lens surfaces were held spherical (as in Epps 1989a,b) throughout. The on-axis performance of the final design as a function of wavelength is shown in Fig. 3 for a single pass through the lens system. Note from Fig. 3(b) that chromatic aberration is corrected at three wavelengths, and the residual tertiary chromatic aberration is ± 75 μm from $\lambda = 4000$ Å to nearly 1.1 μm. Spherochromatism, the variation of spherical aberration with wavelength, can be seen from the dotted curve in Fig. 3(a) which represents the rms image diameter at the individual best focus for each wavelength; spherical aberration is corrected for Fraunhofer F light (Hβ), where the lens design gives essentially diffraction-limited performance. The solid curve in Fig. 3(a) shows the expected performance without refocus, while the dashed lines indicate the 27 μm pixel size of the Reticon CCD (recall that the slit projects to two CCD pixels) as well as a 15 μm pixel size for comparison purposes. Typically the rms image diameter is 10–15 μm.

Off-axis performance is nearly identical to Fig. 3 out to a 20 mm field radius. Beyond a 30 mm radius off axis, the correction for field curvature breaks down and rms image diameters (still $\leqslant 20$ μm at 30 mm off axis) on the flat focal plane begin to degrade rapidly. The clear aperture of the CCD Dewar window field flattener was therefore set at 60 mm. The CCD mounting base design is an adaptation of the Palomar system (Gunn et al. 1987), modified for the Reticon 1200×400 CCD, IR Labs ND-2 Dewar (stretched to 3 ℓ capacity), and the new McDonald Observatory CCD electronics system (Kaiser et al. 1992; Paper II).

Recall from Fig. 2 and Sec. 3.1 that light from the spectrograph slit enters the camera lens system after reflecting from an off-axis folding mirror (see inset). Since the CCD is centered on the optical axis of the camera (as is β_c, defining the blaze peak or centers of the echelle orders), the input slit image is $2\theta = 2.31°$ off axis as seen through the camera from the grating. The bottom edge of the folding mirror is beveled so as not to occult any of the light bound for the CCD from the spectrograph camera, while attempting to minimize $\alpha - \beta_c$. An off-axis segment of a spherical field-flattener-like corrector lens, whose surface radii we optimized specifically for the off-axis location of the slit, is interspersed between the slit and the folding mirror, and the alignment of the corrector lens and mirror determined based on the deviation of the chief ray through the lens (as calculated from the raytrace). The clear aperture of the off-axis corrector lens segment is 19×44 mm, the long axis

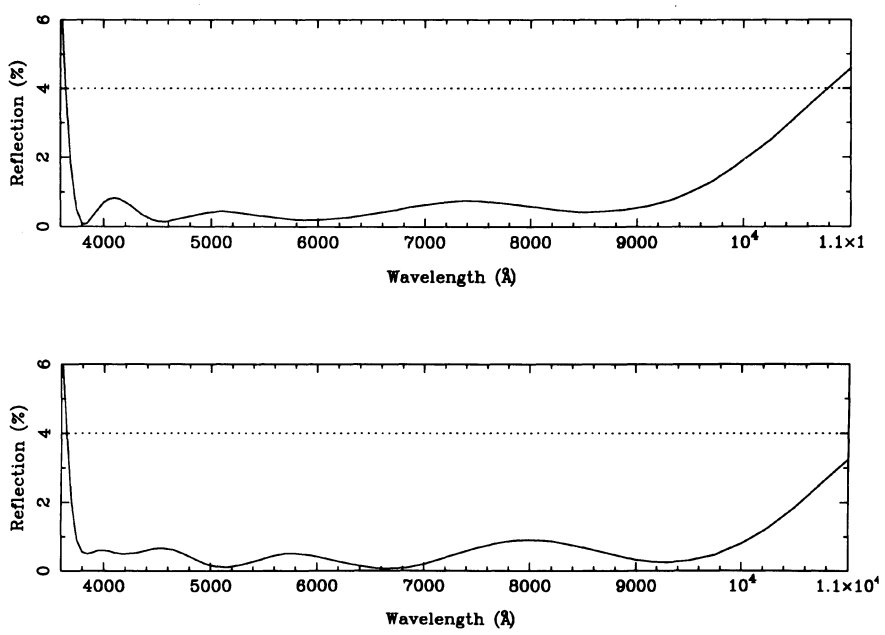

FIG. 4—Reflection loss as a function of wavelength measured from witness samples to the AR coating applied to all custom optics in the spectrograph. Top: coating optimized for refractive index $n=1.47$ substrate. Bottom: coating optimized for higher index $n=1.57$ substrate.

parallel to the slit jaws (tangential in the field of view of the camera). Camera plus corrector off-axis image quality along a 30 mm slit length is again 15 μm or less, and the image quality remains quite acceptable for 2–3 mm outward from the optical center of the corrector, and for 6 mm or more inward; these limits would define the field boundaries of any potential future multislit assembly (Sec. 3.6 below).

The outer surfaces of the camera triplet and doublet lenses, both surfaces of the fused quartz field flattener, off-axis corrector, and LF5 prism have been antireflection coated with a very broadband coating by Continental Optical. Shown in Fig. 4 are reflection losses as a function of wavelength measured from witness samples of different refractive indices. From 3700 to 9500 Å the average reflectivity of the coated surfaces is approximately 0.5%. Due to the large thermal expansion coefficients of CaF_2 and FK01 lens materials, the large triplet and doublet have been cemented together with Dow Corning Sylgard 184 and Prime Coat, a flexible, optically transparent two-part silicone elastomer. After one year under ambient conditions at the observatory, no evidence of separation has been seen at any of the cemented interfaces.

3.3 Preslit Optics

The conversion from the $f/13.5$ telescope input beam to an $f/5$ beam at the slit input to the spectrograph camera lens system is accomplished in our design using a pair of stock photographic lenses, each at infinite conjugate. At one focal length distance (35 mm Nikon cameras share a common back focal length of 46.5 mm as measured from the bayonet lens mounting surface) below the $f/13.5$ telescope focus a 135 mm EFL $f/3.5$ Nikkor lens "collimates" the beam producing a 10 mm diam pupil. Below the pupil a 50 mm EFL $f/1.4$ Nikkor lens reimages the telescope field on the slit at $f/5$. Image scale at the slit equals 50.5 μm per arcsec at the reimaged 2.1 m Cassegrain focus, a spot size which is well within the resolving power of this pair of Nikon lenses. We felt it was important that the slit follows these reimaging optics so that any aberrations which might give rise to on-axis images greater than 50 μm in size would result primarily in increased slit losses rather than poorer spectral resolution on the CCD. No such aberrations have been observed, however.

While 35 mm photographic lenses may not be optimum for astronomical applications in which the absolute maximum throughput is desired, their use here offers us a potentially large degree of versatility. Interchanging the 135 mm lens for one of a different focal length is equivalent to changing the collimator effective focal length of the spectrograph, as, for example, when one wishes to accept a different output $f/$ratio from a fiber-optic feed. Furthermore, it will be possible at any future time to replace the commercial photographic lenses with more efficient custom designs having fewer and more UV-transmissive optical elements in exchange for inconsequential sacrifices in spot sizes and field (the crossed-dispersed echelle spectrograph works exclusively on axis).

3.4 Slit and Field Viewing Optics

With the instrument at Cassegrain it is necessary to image a wide field (1 arcmin minimum) for object acquisition and alternately guide the telescope remotely using light reflected off the slit jaws. With the reimaging system described above, the latter had to be accomplished in a somewhat unorthodox way if gross tilts of the slit plane

were to be avoided. Our approach, which has proven relatively successful, was to tilt the slit plane by only 6.52° so that light reflected by the slit jaws returns through the 50 mm $f/1.4$ Nikkor lens above the slit. Owing to the tilt, however, the returning rays will pass through a 10 mm pupil which is 11.6 mm offset from the pupil formed of incoming rays by the 135 mm lens. A small pickoff mirror located at the returning ray pupil intercepts the reflected light from the slit jaws without occulting any of the incoming rays, and sends the intercepted rays to a pair of relay mirrors which together route this light (collimated by its return through the 50 mm lens above the slit) to a 70–210 mm Nikon autofocus zoom lens and CCD-based TV guider camera. This provides for remote slit viewing and guiding.

All three of these pickoff and TV guider relay mirrors are fixed to a rotating stage, another position of which carries instead a single mirror which intercepts the incoming light collimated by the 135 mm lens and diverts it directly and entirely to the CCD-based TV guider camera for field viewing. Although there has been no change in net TV image scale, this mode is without interference from the relatively nonreflective decker which covers the slit, nor does focus degrade away from the center of the screen as happens in the slit viewing mode (since the slit itself is tilted while the 50 mm $f/1.4$ lens above the slit is not). The TV guider lens zoom is manually adjusted for the best compromise between field of view and detail necessary for accurate guiding. Our plan with a second-generation CCD-based TV guider system upgrade is to implement a "software zoom" magnified pixel display for ease of guiding while at the same time a larger field of view for object acquisition.

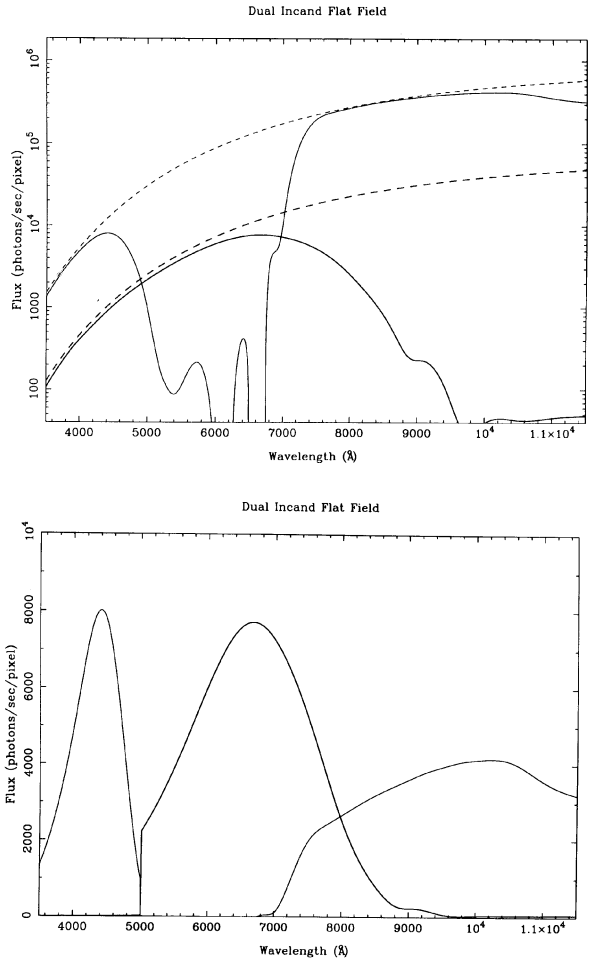

FIG. 5—Theoretical flat-field flux from the system of two lamps, two filters, and dichroic beamsplitter described in the text. Top: upper curves show 60 W lamp before (dashed) and after (solid) 3 mm BG-3 filter; lower curves are for a 5 W lamp before and after 3 mm KG-3 filter. Bottom: flat-field photon fluxes on a linear scale when combined by a $\lambda = 5000$ Å dichroic beamsplitter.

3.5 Calibration Lamps

An additional benefit resulting from the pair of reimaging lenses above the slit concerns the internal 10 mm diam pupil found between them. Light emanating from a 10 mm diam ground glass screen located at the position of this pupil is imaged by the 50 mm lens above the slit such that it illuminates the subsequent spectrograph optics in exactly the same way as does incoming starlight. The rotating stage which carries the relay mirrors for the slit- and field-viewing TV guider modes also therefore carries two ground glass and mirror assemblies which accept input from a Th-Ar hollow cathode lamp (for wavelength calibration) or a pair of quartz halogen incandescent lamps (for flat-field calibration), respectively.

Providing a sufficiently uniform source of flat-field illumination for an astronomical echelle spectrograph (especially one with a large wavelength coverage) is difficult owing to the decrease in the $T_{\rm eff} \leqslant 3000$ K Planck function for the lamp throughout the visible, along with the increasing dispersion of the echelle grating toward the blue. Extending the work of McCarthy (1988), we equipped the current instrument with a pair of quartz halogen lamps of greatly differing intensities. To provide sufficient blue and UV photons, one lamp is 60 W and has a 3 mm BG-3 filter in front of it. Light from this lamp reflects off a dichroic beamsplitter and is imaged onto the 10 mm ground glass screen for the flat field. The dichroic transmits longward of 5000 Å, and thus reduces by approximately 10^{-2} the intensity of the red leak through the BG-3 filter, but given the Planck function of the high-wattage bulb, this red light is comparable in intensity with the unattenuated $\lambda < 5000$ Å light at wavelengths longward of 7000 Å. Flat-field flux for 5000 Å $< \lambda < 7000$ Å is provided by a low-wattage (5 W) quartz halogen lamp with a 3 mm KG-3 color balancing filter in front of it; light from this bulb is transmitted by the dichroic beamsplitter for $\lambda > 5000$ Å and simultaneously imaged onto the ground glass screen. Figure 5 contains the results of a computer simulation to predict the flat-field intensity in photons s^{-1} $pixel^{-1}$ resulting from this and other two-bulb/two-filter/dichroic-beamsplitter incandescent lamp design combinations.

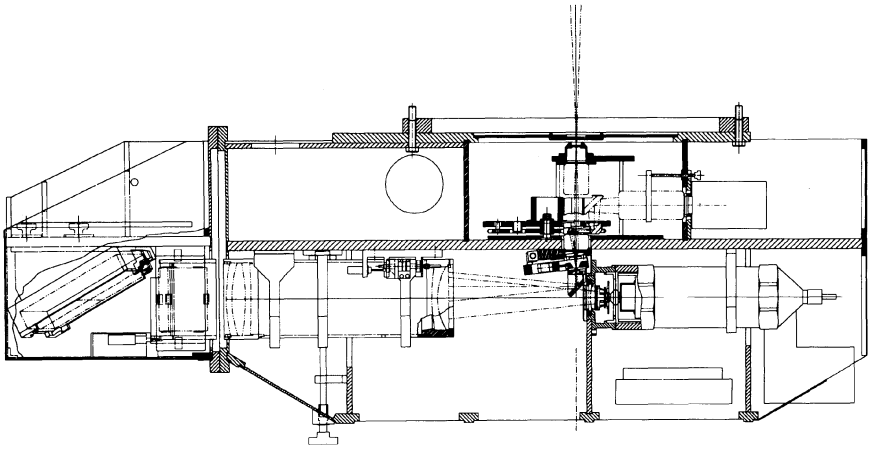

FIG. 6—An engineering cross-sectional view of the spectrograph mechanical design layout. Mechanisms are provided for camera focus, prism tilt, grating wavelength setting, CCD axial tilt, slit width and decker length, slit rotational tilt, guider/lamp stage rotation, TV guider lens zoom, 50 mm square filter insertion, and an entrance dark slide.

3.6 Alternate Modes of Operation

As mentioned above, one possible alternate mode of operation for this new cross-dispersed echelle spectrograph is coupled to the Cassegrain focus via a fiber-optic cable. To operate in this mode, the 135 mm EFL Nikkor lens can be replaced by a shorter focal length Nikkor lens appropriate to the diameter and output f/ratio of the fiber, and the fiber itself positioned at the top of the spectrograph in what had been the telescope focal plane. The fiber could then be translated in that plane, until by monitoring with the TV guider in the slit-viewing mode, it is observed to be aligned with the spectrograph slit. The slit could be open to the reimaged size of the fiber or closed smaller (e.g., to maintain two pixel resolution for a larger-diameter fiber feed offering greater throughput) depending upon the most efficient combination of fiber diameter, throughput, focal ratio degradation, and reimaging demagnification found (Ramsey 1988; McCarthy 1989). While one would ordinarily take flat-field and Th-Ar exposures through the fiber fed from its input end, the capability of using the internal flat-field lamp assembly described above (together with a decker setting larger than the fiber diameter) in addition would effectively guard against drifts of the fiber spectra perpendicular to the echelle dispersion with time.

Equally attractive is an alternate mode (following McCarthy 1988, 1989) in which the echelle grating and prism cross disperser are replaced by an ordinary grating for lower-dispersion, single-order, long-slit spectroscopy, taking advantage of the high throughput efficiency and state-of-the-art CCD performance available with the new Cassegrain (echelle) spectrograph. In the absence of the echelle grating and LF5 prism, the collimator and camera beams will intersect on the camera optical axis approximately 400 mm in front of the vertex of the first camera surface. A large grating such as those found in the 2.1 m coudé spectrograph (150×200 mm, 600 or 1200 gr mm^{-1}) at this location would operate at lower dispersion with the same $\alpha-\beta_c=2\theta=2.31°$ optical configuration as the echelle, minus the prism. Resolutions ranging from 24,000 down to 4000 could be achieved using existing gratings, and down to $R=1000$ with coarser low blaze angle gratings available from Milton Roy. The 400 pixel dimension of the Reticon CCD perpendicular to the dispersion would project to a maximum slit length of 200 arcsec on the sky. For this reason we incorporated a provision for user-installed 50 mm square filters in the parallel beam above the slit, possibly to be used in the future for order separation with low-dispersion gratings. Likewise the decker jaws will open to reveal a 10 mm long slit, and stationary decker masks can even be removed to achieve a full 30 mm slit length, which all optical elements (except currently the CCD detector) were designed to accommodate. Provision for a field lens in the telescope focal plane exists for this purpose also, although it is not required for point-source observations using the cross-dispersed echelle spectrograph mode.

4. SPECTROGRAPH MECHANICAL DESIGN

4.1 Structural Overview

To optical design layout shown in Fig. 2 and described above is housed in a large aluminum structure made of half inch (12.7 mm) thick plates of 6061-T6 aluminum alloy, with all optical subassemblies attached to a central 1 in. thick aluminum midplane. Figure 6 is an engineering cross section of the assembled instrument. Noteworthy from this view is the large bolt circle diameter (0.86 m) for attaching the instrument to the telescope. Owing to the large spectrograph weight expected, we chose to bolt directly to the rotating Cassegrain ring on the telescope in place of the 250 kg cast iron Cassegrain "tailpiece" to which all other 2.1 m Cassegrain instruments attach, saving this extra weight (plus its declination and R.A. counterweights) and

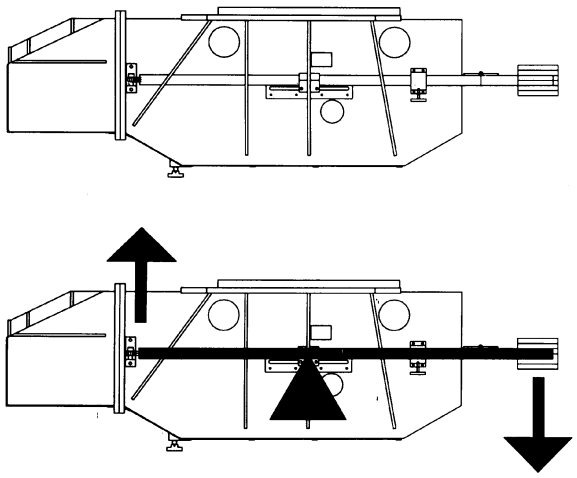

FIG. 7—Cantilever principle employed in this spectrograph design to reduce the amount of gravitational flexure experienced at Cassegrain. Weights suspended at right are to balance the instrument around the telescope optical axis; owing to the cantilever arrangement, they apply an upward force counter to gravity at the left side where the camera optics and dispersing units are located.

providing us the maximum possible bolt circle diameter. Total weight of the 2.1 m Cassegrain echelle spectrograph is approximately 550 kg.

Also visible in Fig. 6 is the large flange between the front of the camera and the cross-dispersing prism, which permits the prism and echelle grating "dispersion unit" section of the spectrograph to be removed and exchanged for some other "dispersion unit" designed for long-slit, low-dispersion spectroscopy, for example. As mentioned previously the slit jaws are over 30 mm in length, and provision exists for observers to install 50 mm square filters for order separation. As of this writing no definite plans exist for a second dispersion unit, but with a view to the future we felt it was very important to allow for this capability.

4.2 Flexure Compensation

It is apparent from Figs. 2 and 6 that the spectrograph extends a large distance (1.5 m) radially outward from the telescope optical axis along the underside of the telescope. Even with the large (0.43 m) bolt circle radius, tall side walls, and gusset stiffeners [Fig. 7(a)], there was ample reason to be concerned about gravitational flexure at the Cassegrain focus. We therefore added a unique flexure compensation feature to the spectrograph design: given the spectrograph optical layout, it was clear that some form of counterweight would be necessary to balance the instrument on the rotating Cassegrain ring about the telescope optical axis. However, by suspending this dead weight on pivots near the midpoint of the spectrograph, an upward force could be applied to counter gravitational flexure at the dispersion unit end of the instrument [Fig. 7(b)].

In order to determine the optimum cantilevered force required, we modeled the cross-sectional structure of the spectrograph as a function of x, measured along the spectrograph optical axis with $x=0$ at the midpoint of the spectrograph below the telescope optical axis. For the telescope at the zenith ($+z$-axis), gravitational flexure would tend to bend the dispersion end of the instrument in the $-z$ direction an amount governed by the relationship

$$\frac{d^2z}{dx^2}=\frac{M(x)}{EI(x)}, \tag{3}$$

where $M(x)$ is the bending moment exerted by gravity as a function of distance x along the spectrograph axis, including both the weight of point loads (grating, prism, camera, etc.) and the distributed weight of the structure itself,

$$M(x)=\sum_i W_i(x_i-x). \tag{4}$$

E in Eq. (3) is the modulus of elasticity for aluminum (10^7 psi), and $I(x)$ is the moment of inertia of the spectrograph structure cross section about its neutral axis z_0. For a structure cross-sectional element $dA=dy\,dz$,

$$I(x)=\int_A dI=\int (z-z_0)^2\,dA=\int (z-z_0)^2\,dy\,dz, \tag{5}$$

where the neutral axis of the structure cross section is defined by

$$z_0=\frac{\int z\,dy\,dz}{\int dy\,dz} \tag{6}$$

as a function of x. Figures 8(a) and 8(b) show $I(x)$ and $M(x)$ determined for our final spectrograph structure design. The first integral of Eq. (3) for dz/dx, or the slope due to flexure, is actually much more important in our application than the second integral for displacement, since the light is collimated when striking the grating and returning to the camera. One CCD pixel (2.5 km s^{-1} in velocity units) subtends of order 7 arcsec in the field of the camera as seen from the grating, and thus a flexure induced tilt at the grating of 1 arcsec would shift the diffracted image 2 arcsec, or over $\frac{1}{4}$ pixel on the CCD (0.6 km s^{-1}).

Flexure compensation aside, the spectrograph structure was designed to be as stiff as possible given the weight and size limits for the 2.1-m telescope. Nevertheless, flexure in excess of $\frac{1}{4}$ pixel would be experienced from the structure itself (in addition to flexure from any internal components) were it not for the cantilevered action of the counterweight. By appropriate choices of the counterweight mass, distance from the telescope optical axis (the product being fixed by the requirement that the counterweight furnish rotational balance on the Cassegrain ring), and cantilever pivot point, it is possible to very nearly eliminate the flexure-induced tilt of the dispersion unit. Figures 8(c) and 8(d) demonstrate this cancellation with plots of $\theta(x)=dz/dx$ and $z(x)$, respectively, where the cantilevered action of the counterweight has been included in Eqs. (4) and (3) above.

As implemented (see photographs in Fig. 9), the pivot points can be moved ± 6 in. (150 mm) to adjust the amount of upward force applied to the dispersion unit

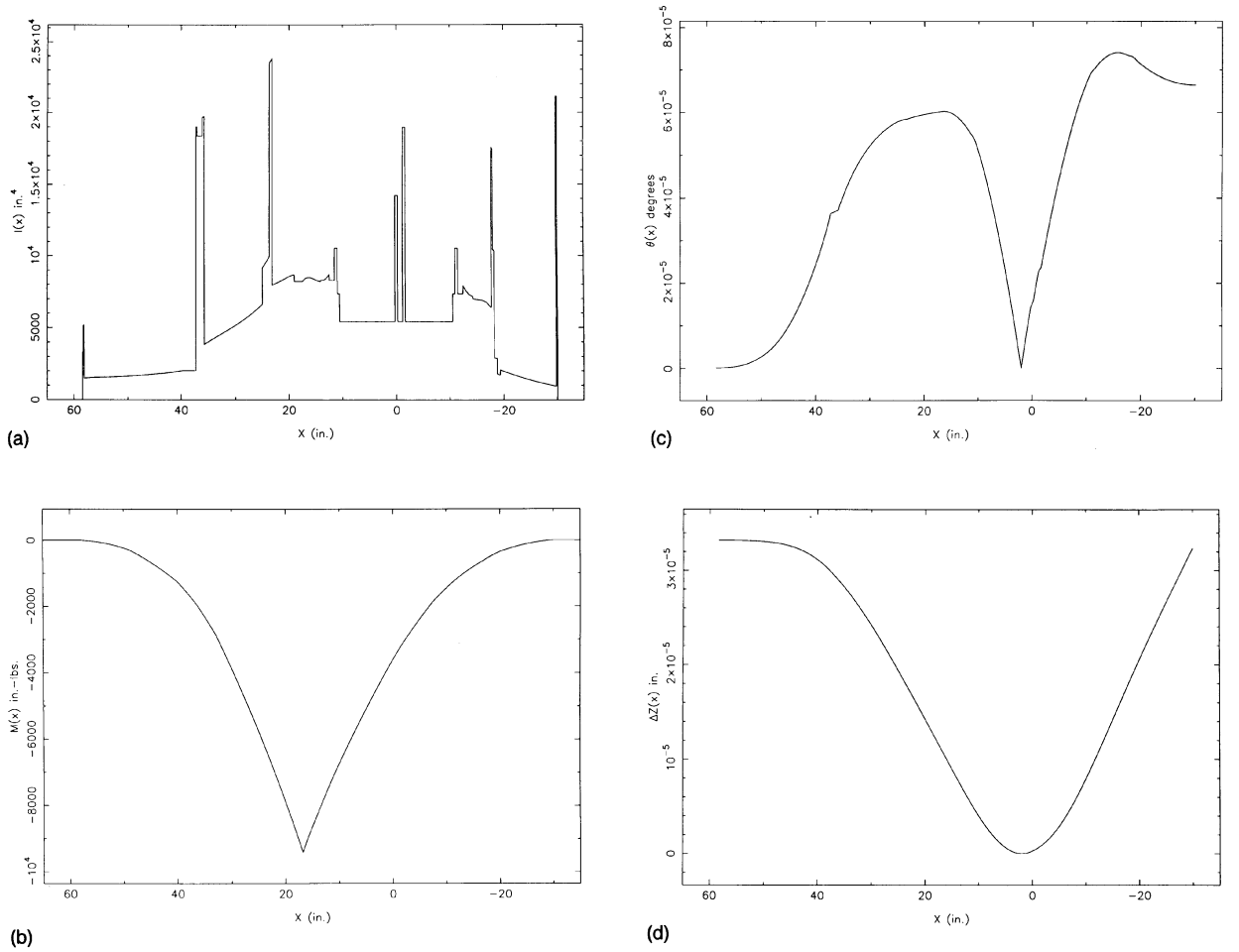

FIG. 8—Variation of (a) cross-sectional moment of inertia and (b) bending moment for the spectrograph without flexure compensation. With flexure compensation, the resulting (c) slope and (d) displacements due to gravity.

flange. The pivots themselves are cylindrical rings, so that the force they exert on the counterweight arms is always radial and in a vertical plane regardless of the orientation of the instrument.

5. SPECTROGRAPH PERFORMANCE

5.1 Flexure

The spectrograph first became operational in 1991 August and was observed to suffer from a much greater amount of gravitational flexure (in excess of 1.0 pixel) than expected on theoretical grounds. After several months we had eliminated and/or ruled out movement of the CCD inside the Dewar or the camera on its crossed roller bearings as possible causes, along with the slit, folding mirror, prism, and echelle grating mounts. Only after adding stiffening supports to the top of the 1.0 in. plate in the dispersion unit were we able to significantly reduce the gravitationally induced flexure to a negligible level. Currently the worst-case flexure shift observed over 60° (4 h) of telescope motion is 0.3–0.4 pixels. However, if the recommendation that the Cassegrain ring rotation angle be set to align the slit with the direction of atmospheric dispersion (Filippenko 1982) is followed, flexure in this orientation is considerably less (0.1–0.2 pixels over 60°, or 4 h). Investigations will continue on cloudy nights aimed at isolating and subsequently eliminating the flexure still present. We do not believe the flexure-compensated structure is itself responsible for this flexure, since the flexure shift does not reverse sign at the zenith. Rather, some internal component is not sufficiently stiff—the flexure which remains does seem perfectly elastic, however, and is presumed to originate from something bending, not from the movement of something which is loose.

5.2 Optical Image Quality

The performance of the spectrograph camera design has met all expectations, and for a narrow slit width the optics will indeed produce ~1 pixel FWHM Th-Ar image profiles. More importantly, the focus seems reasonably uniform across the CCD focal plane considering that the CCD itself is a thinned, backside-illuminated edge-supported membrane, and is far from absolutely flat. Variation of camera focus with wavelength is small and can generally be

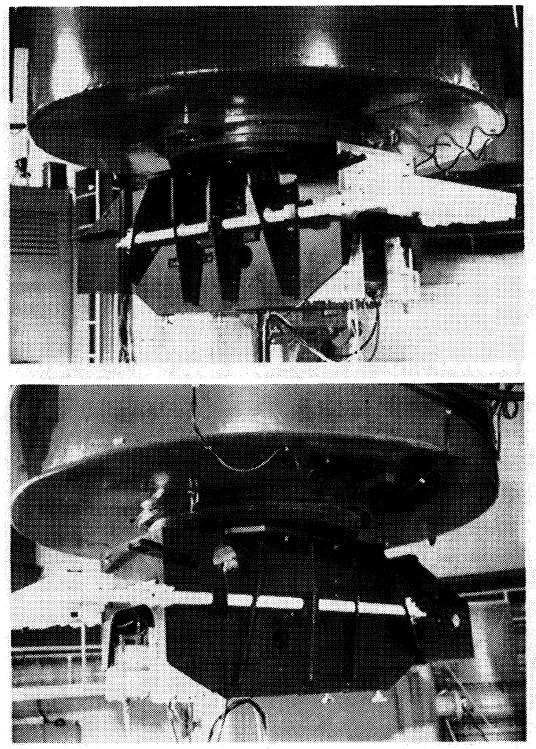

FIG. 9—Two views of the spectrograph attached to the Cassegrain focus of the 2.1 Struve reflector at McDonald Observatory. The flexure compensation cantilever system can be seen in white.

neglected. Scientific observations with the 2.1 m Cassegrain echelle spectrograph began in the summer quarter of 1992 with a science-grade CCD on loan from Lick Observatory (we still await our final science-grade chip from Reticon).

In actual practice, a slit width of 1.0 arcsec (50 μm at the reimaged $f/5$ focal plane in which the slit is located) results in 2.0 pixel (54 μm) FWHM line profiles on the CCD detector. The reciprocal dispersion at Hα is 0.05525 Å pixel^{-1}, giving a spectral resolution times slit width product of 59,400 arcsec. Figure 10 shows two example echelle orders from the star Mu Leonis ($V=3.9$, $Sp=$K2 III, exposure time$=270^{s}$) demonstrating the $R\simeq 60{,}000$ spectral resolution provided by the instrument.

The ability to accurately flat-field calibrate stellar spectra with the coarse 23.2 gr mm^{-1} R2 echelle grating has not proved to be a problem in practice, although we have found it necessary to background subtract the flat-field exposures in order to properly remove the echelle grating blaze profile from stellar exposures. We attribute this background in the flat fields to the out-of-focus decker jaws above the slit (see below) and hope to have this problem corrected in the near future.

The scattered light level is very low for stellar spectra in good seeing (interorder minima approximately 1% of order peak intensity), even in the red where the order-to-order spacing is near its minimum. Figure 11, kindly provided by Dr. Verne Smith, compares equivalent width measurements of Arcturus taken with this instrument in the 6100–6800 Å region to those measured from the Arcturus atlas (Griffin 1968) of Mt. Wilson 100 in. (2.5 m) coudé spectra. The agreement is well within the accuracy of the measurements, verifying the absence of any significant scattered light problem in the echelle.

As mentioned above our unorthodox slit-viewing optics design has proven to be successful, although again we have spent the first year with an earlier generation CCD-based TV guider camera than the newer, more sensitive model we have been expecting from the manufacturer. Two minor problems exist with the decker mechanism: more backlash exists in its motion than we would like, and the decker jaws sit slightly above the slit jaws (to avoid scratching the polished reflective surface of the slit jaws). In the relatively fast $f/5$ beam at the slit, this results in the decker-defined edges of the orders in, for example, flat-field exposures being rounded and "soft" since the decker jaws are out of focus as seen from the CCD detector. We expect to have these minor problems solved over the coming months.

CCD spectra obtained with the Sandiford 2.1 m Cassegrain echelle spectrograph suffer from the presence of a series of bright slit images (somewhat elongated in the echelle dispersion direction). These artifacts are nearly centered on the CCD in the cross-dispersion direction (in general not aligned with any echelle order) and usually appear to one side of center in the echelle dispersion direction. They are also present in the CCD spectra obtained with the large new prism cross-dispersed white pupil echelle spectrograph of the McDonald 2.7 m coudé (Tull et al. 1993). The origin of this feature, dubbed the "picket fence," has been thoroughly investigated by Tull and is now understood to be light which has reflected from the CCD detector and returned through the camera and prism to the grating. There it is once again dispersed—the returning light strikes the grating at an incident angle α' approximately equal to the original grating angle β, but order number m' may differ from the original order m—and is imaged back onto the CCD by the camera. We refer the reader to the forthcoming paper by Tull et al. (1993) for a more detailed explanation, here noting only that it is the combination of $\gamma=0$ and small θ (i.e., grating geometry very near to true Littrow) which permits this reflected light to again return to the CCD. The impact of the "picket fence" on echelle spectra obtained with the 2.1 m Cassegrain instrument is that a third of the wavelength range of one or (more commonly) two echelle orders in the center of the CCD is obscured by these bright artifacts.

5.3 Throughput Efficiency

Three 1000^{s} exposures of the secondary standard star HD 19445 (Oke and Gunn 1983) were taken on 1992 August 5 (U. T.) in good seeing. The total counts above background at $\lambda=5900$ Å averaged 32,600 DN per pixel in the dispersion direction, with the CCD gain set at $3e^{-}$/DN. Taking $AB_{79}(5900\text{ Å})=7.93$ for HD 19445, we derive a total system throughput of 10% from above the atmosphere, through the telescope, slit, spectrograph, and

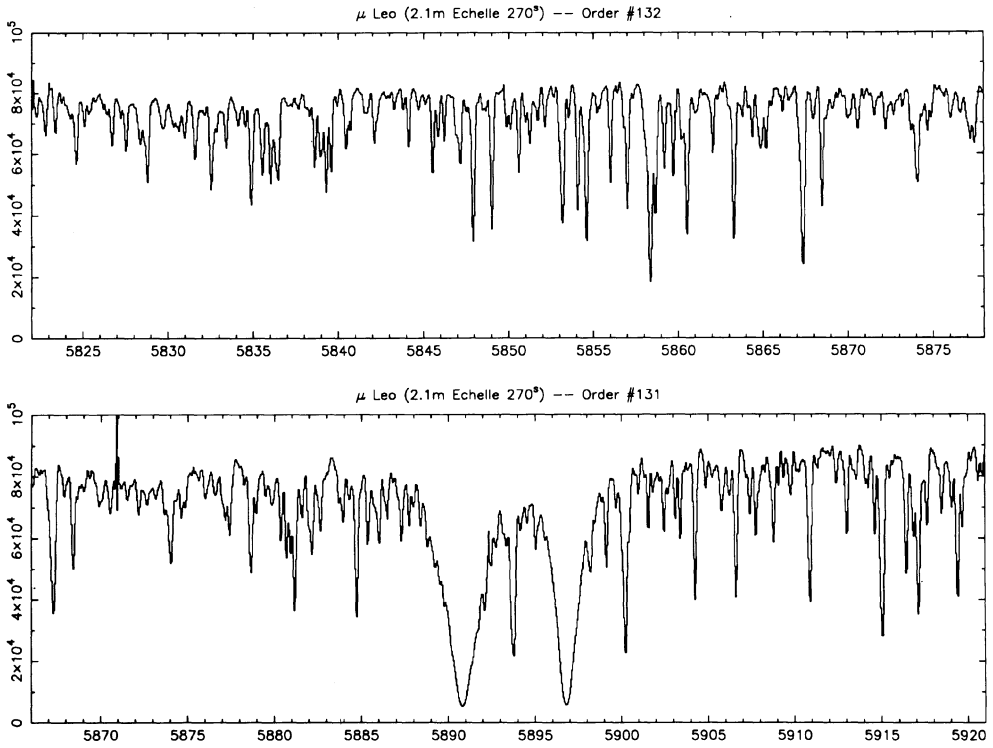

FIG. 10—Two sample echelle orders from a 270^s total exposure time sum of μ Leo (V=3.9; Sp=K2 III) spectra taken with the instrument described in this paper. These data have been background subtracted and flat fielded, but otherwise unretouched; a continuum slope may exist from differences in color temperature between the star and flat-field lamp.

CCD detector. The measured S/N ratios from the spectra are consistent with this photon flux, and the 10% throughput compares favorably with the 11% peak efficiency of the Palomar 1.5 m echelle spectrograph (McCarthy 1988).

Just as the throughput efficiency of the Palomar 1.5 m echelle was recently increased to 17% with the installation of an antireflection coated CCD (Lesser 1991), work is currently in progress to AR coat the thinned Reticon 1200 $\times$400 CCD for the Sandiford 2.1 m Cassegrain echelle spectrograph. In addition to increasing the total throughput efficiency into the 15%–20% range, this will decrease the intensity of the picket fence artifact by perhaps 80% since the fraction of light reflected from the CCD will decrease from roughly 50% to 10%.

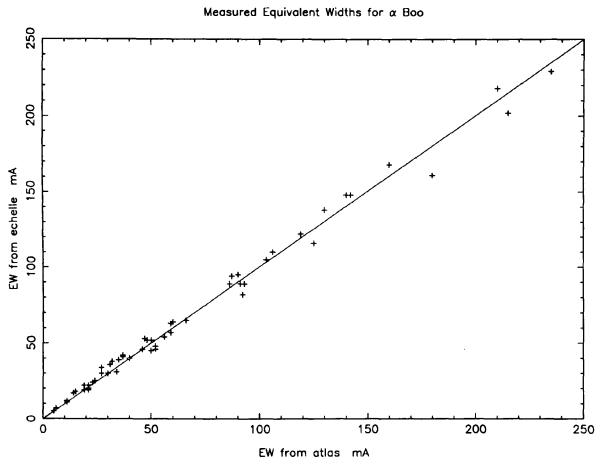

FIG. 11—A comparison between equivalent widths of absorption lines in the $\lambda\lambda$6100–6800 Å region of α Boo, as measured from spectra obtained with the Sandiford echelle vs. identical measurements from the Arcturus atlas (Griffin 1968); agreement is within the accuracy of the measurements. Data courtesy of Dr. Verne V. Smith, University of Texas at Austin.

It is a pleasure to thank David L. Lambert and his co-workers at U. T. Austin for providing a stimulating scientific climate in which this instrument project could germinate and mature, and for many enlightening discussions and advice. Verne V. Smith is due special mention in this regard along with gratitude for his active role in instrument commissioning and use since spring 1992 and for permission to include his Alpha Boötis equivalent width comparison data. We also wish to thank Frank Bash, Thomas G. Barnes III, the late Harlan J. Smith, and members of the McDonald Observatory Council and Mt. Locke staff for their indulgence and assistance throughout this undertaking. Funds were provided to David Lambert by the Dean of the College of Natural Sciences, U. T. Austin, and by the Robert A. Welch Foundation and NSF AST 89-02835, and are gratefully acknowledged.

We also are grateful for the unselfish and untiring assistance of Mary Beth Kaiser, Philip MacQueen, J. Fred

Harvey, and Doug Edmonston regarding the CCD and instrument electronics incorporated into this spectrograph. The skilled craftmanship of machinists Jimmy Welborn, George Barczak, and Tom Phillips is reflected in the finished product and is greatly appreciated. We are indebted to Sam Odoms for providing software support so crucial during the commissioning phase of a new instrument such as this. It gives us pleasure to thank Gordon Wesley for his recent and continuing mechanical assistance as the new Project Engineer, and we look forward to his many future contributions both to this instrument and to the Observatory. Congratulations are extended to Bob Tull, Phillip MacQueen, and John Good on the nearly simultaneous successful completion of their large 2.7 m coudé echelle spectrograph; we feel most fortunate to have had many open exchanges of ideas and experiences with those involved in that effort.

We wish to thank Stephen Shectman and Harland Epps for lending us their creative and insightful suggestions, and for permission to cite unpublished work. The timely, conscientious, and careful supervision over critical optical fabrication by Stephen Fantone of Optikos Corporation (main $f/5$ camera system), Paul James of Continental Optical (broadband AR coatings), and Anthony Marino of Glass Fab Inc. (LF5 prism) is gratefully acknowledged. Also appreciated are the good faith efforts by Tom Blasiak and co-workers at Milton Roy (echelle grating), Bob Maddoux and co-workers at Reticon (scientific CCDs), and Bill Simon and Bob Harwell of MicroLuminetics (CCD-based TV guider camera); we look forward to receiving the final fruits of these efforts in the near future.

The 2.1-m Cassegrain echelle spectrograph described here has been respectfully dedicated to the memory of our good friend and colleague, **Brendan A. Sandiford** (1949–1992), who served energetically as Project Engineer beginning in early 1990. His experience, enthusiasm, and eagerness to learn will long be remembered by those who had the pleasure of knowing him and working with him.

REFERENCES

Bardas, D. 1977, PASP, 89, 104
Barden, S. C. 1988, in Instrumentation for Ground-Based Optical Astronomy, Proceedings of the 9th Santa Cruz Summer Workshop, ed. L. B. Robinson (New York, Springer), p. 250
Chaffee, F. H., Jr., and Latham, D. W. 1982, PASP, 94, 386
Cizdziel, P. J. 1990, in ASP Conference Series No. 8, CCDs in Astronomy, ed. G. Jacoby, p. 100
Diego, F. 1988, in Instrumentation for Ground-Based Optical Astronomy, Proceedings of the 9th Santa Cruz Summer Workshop, ed. L. B. Robinson (New York, Springer), p. 6
Diego, F., Charalambous, A., Fish, A. C., and Walker, D. D. 1991, Proc. SPIE, 1235, 562
Enard, D. 1982, Proc. SPIE, 331, 232
Epps, H. W. 1989a, Preliminary 24.0 Inch $f/3.0$ Camera Lens Design Alternatives for a Littrow Echelle Spectrograph, unpublished report, 12 June 1989
Epps, H. W. 1989b, private communication. Our optical design is a refinement of OARSA Run No. 6610, 30 September 1989
Filippenko, A. V. 1982, PASP, 94, 715
Geary, J. C., Torres, G., Latham, D. W., and Wyatt, W. F. 1990, in ASP Conference Series No. 8, CCDs in Astronomy, ed. G. Jacoby, p. 40
Gehren, T. 1990, in Proceedings of the 2nd ESO/ST-ECF Data Analysis Workshop, ed. D. Baade and P. J. Grosboel, p. 103
Gilmore, D. K., Robinson, L. B., Stover, R. J., Brown, W. E., and Wei, M. 1990, in ASP Conference Series No. 8, CCDs in Astronomy, ed. G. Jacoby, p. 116
Griffin, R. F. 1968, A Photometric Atlas of the Spectrum of Arcturus $\lambda\lambda$3600–8825 Å (Cambridge, Cambridge Philosophical Society)
Gunn, J. E., Emory, E. B., Harris, F. H., and Oke, J. B. 1987, PASP, 99, 518
Hiltner, W. A. 1949, private communication (item 16 of Table 3, and Fig. 3) to Bowen, I. S. 1960, Astronomical Techniques, ed. W. A. Hiltner (Chicago, University Chicago), p. 34
Kaiser, M. E., Edmonston, R. D., McCarthy, J. K., Harvey, J. F., and Opal, C. B. 1992, BAAS, 24, 691
Lambert, D. L. 1991, in Evolution of Stars: The Photospheric Abundance Connection, ed. G. Michaud and A. Tutukov (Dordrecht, Kluwer), p. 299
Lesser, M. P. 1991, Proc. SPIE, 1447, 177
le Luyer, M., Melnick, J., and Richter, W. 1979, ESO Messenger, 17, 27
Loewen, E. G. 1988, in Instrumentation for Ground-Based Optical Astronomy, Proceedings of the 9th Santa Cruz Summer Workshop, ed. L. B. Robinson (New York, Springer), p. 118
MacQueen, P. J., and Tull, R. G. 1988, in Instrumentation for Ground-Based Optical Astronomy, Proceedings of the 9th Santa Cruz Summer Workshop, ed. L. B. Robinson (New York, Springer), p. 52
McCarthy, J. K. 1985, Proc. SPIE, 554, 155
McCarthy, J. K. 1988, Ph.D. thesis, California Institute of Technology
McCarthy, J. K. 1989, The Optical Design of an 82-inch Cassegrain and 36-inch Fiber-fed CCD Echelle Spectrograph for the McDonald Observatory, December 1989 internal report, unpublished
Oke, J. B., and Gunn, J. E. 1983, ApJ, 266, 713
Pilachowski, C., Sneden, C., Dominy, J. F., Cottrell, P., and May, D. C. 1982, PASP, 94, 1029
Ramsey, L., and Huenemoerder, D. 1986, Proc. SPIE, 627, 282
Ramsey, L. W. 1988, in ASP Conference Series No. 3, Fiber Optics in Astronomy, ed. S. C. Barden, p. 26
Robinson, L. B., Brown, W., Gilmore, K., Stover, R., and Wei, M. 1991, Proc. SPIE, 1447, 214
Schroeder, D. J. 1967, Appl. Opt., 6, 1976
Schroeder, D. J. 1970, PASP, 82, 1253
Schroeder, D. J. 1988, in Instrumentation for Ground-Based Optical Astronomy, Proceedings of the 9th Santa Cruz Summer Workshop, ed. L. B. Robinson (New York, Springer), p. 39
Shectman, S. A., and McCarthy, J. K. 1983, an unpublished Dupont 2.5 m UV/visible echelle spectrograph design in which an $f/7.5$ quartz/fluorite triplet collimator lens and quartz cross-dispersing prism are both used in double pass, and the faster camera $f/$ratio is produced by a quartz aplanatic sphere just before the detector
Shectman, S. A. 1983–87, private communication, the Dupont 2.5 m echelle as built uses a glass prism cross disperser and 100 mm aperture $f/5$ triplet camera lens in double pass
Smith, H. J. 1991, in ASP Conference Series, No. 20, Frontiers of Stellar Evolution, ed. D. L. Lambert, p. 1

Smith, V. V. 1988, in The Origin and Distribution of the Elements, ed. G. J. Mathews (Singapore, World Scientific), p. 535

Sneden, C. 1991, in Evolution of Stars: The Photospheric Abundance Connection, ed. G. Michaud and A. Tutukov (Dordrecht, Kluwer), p. 235

Tseng, H.-F., Nguyen, B. T., and Fattahi, M. 1989, Proc. SPIE, 1071, 170

Tull, R. G. 1972, in Proceedings of the ESO/CERN Conference on Auxiliary Instrumentation for Large Telescopes, ed. S. Laustsen and A. Reiz, p. 259

Tull, R. G., and MacQueen, P. J. 1988, in Proceedings of the ESO Conference No. 30, Very Large Telescopes and Their Instrumentation, ed. M.-H. Ulrich, p. 1235

Tull, R. G., MacQueen, P. J., Sneden, C., and Lambert, D. L. 1993, PASP, in preparation

Vogt, S. S. 1987, PASP, 99, 1214

Vogt, S. S. 1988, in Instrumentation for Ground-Based Optical Astronomy, Proceedings of the 9th Santa Cruz Summer Workshop, ed. L. B. Robinson (New York, Springer), p. 33

Vogt, S. S., and Penrod, G. D. 1988, in Instrumentation for Ground-Based Optical Astronomy, Proceedings of the 9th Santa Cruz Summer Workshop, ed. L. B. Robinson (New York, Springer), p. 68

Walker, D. D. 1988, in Instrumentation for Ground-Based Optical Astronomy, Proceedings of the 9th Santa Cruz Summer Workshop, ed. L. B. Robinson (New York, Springer), p. 21

York, D. G., Jenkins, E. B., Zucchino, P., Lowrance, J. L., Long, D., and Songaila, A. 1981, Proc. SPIE, 290, 202